DNS of lean premixed turbulent spherical flames with a Flamelet Generated Manifold

By R. J. M. Bastiaans, J. A. van Oijen†, S. M. Martin, L. P. H. de Goey† AND H. Pitsch

1. Motivation and objectives

The present research is concerned with the direct numerical simulation (DNS) and analysis of turbulent propagation of premixed flame kernels. The simulations are direct in the sense that the smallest scales of motion are fully resolved, while the chemical kinetics are solved in advance and parameterized in a table by the method of the flamelet generated manifolds (FGM) (Van Oijen 2002). The state of the reactions are assumed to be directly linked to a single progress variable. The conservation equation for this progress variable is solved using DNS, with the unclosed terms coming from the table. This allows the use of detailed chemical kinetics without having to solve the individual species conservation equations.

Turbulent premixed combustion of gaseous fuels is one of the most important energy conversion processes today, but its physics are not fully understood (e.g. Driscoll 2003). On the one hand a detailed knowledge is required to understand the behavior of the conversion process and the efficiency and formation of pollutants. On the other hand this insight is needed to obtain the parameterizations that are essential in developing accurate models for large scale simulations. One of the most important processes to understand is the physics of turbulent flame wrinkling. Flame wrinkling is very important because it determines both the total flame surface area as well as the local modulation of the mass burning rate.

Here a lean premixed turbulent expanding flame kernel is studied. Lean premixed combustion is becoming the method of choice for ground based gas turbine combustors due to several advantages. The high percentage of air results in complete combustion, reducing emissions of hydrocarbons and carbon monoxide. The excess air also results in lower combustion temperatures and as a consequence low emissions of nitrogen oxides. Therefore, significant research on turbulent premixed combustion has been performed under lean conditions. Some examples of these investigations are the experimental study of Shepherd *et al.* (2002) and the numerical study of Bell *et al.* (2002). The research of Shepherd *et al.* (2002) indicates that even when the smallest turbulent scales are smaller then the flame thickness there is no significant flame front broadening, i.e. combustion remains within the thin reaction fronts regime. This result is confirmed by an analysis of experimental low swirl burner results of De Goey *et al.* (2004). In the numerical experiments of Bell *et al.* (2002), which includes semi-detailed kinetics, it was concluded that flame wrinkling is the dominant factor for increasing the turbulent flame speed.

From a numerical point of view, the setup of a flame kernel is relatively straight forward. There are no walls and due to the expansion of the kernel itself, all boundaries are considered as outflow boundaries. The initial turbulence is decaying, as is the case in

† Combustion Technology, Eindhoven University of Technology, The Netherlands, www.combustion.tue.nl

most practical combustion applications. However, not many researchers have used flame kernels for the study of premixed turbulent combustion. Of particular interest is the research of Jenkins & Cant (2002), Gashi *et al.* (2004) and Thévenin (2004). The latter study is associated with rich flames, which are not addressed here. Jenkins & Cant (2002) studied the evolution of shape parameters in terms of flame normals and curvatures by means of DNS combined with single step chemistry. One of their conclusions is that at low turbulence intensities there is a tendency to favor spherical over cylindrical curvature. In the study of Gashi *et al.* (2004), the numerical simulations of Jenkins & Cant (2002) were extended and supplemented by experimental PLIF observations for both methane and hydrogen combustion at stoichiometric and lean conditions. The result of the study is a qualitatively good agreement between the simulations and experiments.

Combustion at lean premixed conditions, like in ground-based gas-turbines, predominantly takes place in the flamelet and thin-reaction zones regimes of premixed combustion using Peters (2000) definitions. Consequently, this is the starting point for the development of many models. Several flamelet based models have been developed for premixed combustion in the flamelet regime. The first and most well-known models were derived by assuming that the flame-front is infinitely thin (Bray & Moss 1977). An efficient flamelet model is based on the G-equation (Peters 2000). The G-equation is a kinematic equation which can be used to follow the average position, brush thickness and wrinkling of the flame front. Peters very recently extended the G-equation model for combustion in the thin-reaction zones regime. The model is efficient since it is not sensitive to the internal structure of the turbulent flame brush.

Flame stretch is an important parameter that is recognised to have a determining effect on the burning velocity in premixed flames. In the past this effect has not been taken into account in the flamelet approach for turbulent combustion in a satisfying manner. The laminar burning velocity, which is largely affected by stretch, is an important parameter for modelling turbulent combustion. Flame stretch is also responsible for the creation of flame surface area, affecting the consumption rate as well. In the turbulent case, stretch rates vary significantly in space and time. An expression for the stretch rate is derived directly from its mass-based definition by De Goey & Ten Thije Boonkkamp (1999),

$$K = \frac{1}{M}\frac{dM}{dt}, \tag{1.1}$$

where M is the amount of mass in an arbitrary control volume moving with the flame velocity:

$$M = \int_{V(t)} \rho dV. \tag{1.2}$$

On the basis of this definition, a model for the influence of stretch and curvature on the mass burning rate has been developed. In a numerical study by Groot & De Goey (2002), it was shown that this model, with a slight reformulation, shows good agreement with calculations for spherically expanding laminar flames. This formulation, for the ratio of the actual mass burning rate at the inner layer, m_{in}, relative to the unperturbed mass burning rate at the inner layer, m_{in}^0 (for unity Lewis numbers), reads

$$\frac{m_{\mathrm{in}}}{m_{\mathrm{in}}^0} = 1 - \mathit{Ka}_{\mathrm{in}}, \tag{1.3}$$

with the integral Karlovitz number being a function of flame stretch (Eq. 1.1), flame

surface area, σ, and a progress variable, $\mathcal{Y}$,

$$\mathit{Ka}_{\rm in} := \frac{1}{\sigma_{\rm in} m^0_{\rm in}} \left(\int_{s_u}^{s_b} \sigma \rho K \mathcal{Y} ds - \int_{s_{\rm in}}^{s_b} \sigma \rho K ds \right). \tag{1.4}$$

The integrals have to be taken over paths normal to the flame and s_u, s_b and $s_{\rm in}$ are the positions at the unburned side, the burned side and the inner layer, respectively. The flame surface area, σ, is related to the flame curvature, κ, which is related to the flame normals, n_i on the basis of the progress variable, $\mathcal{Y}$,

$$n_i = -\frac{\partial \mathcal{Y}/\partial x_i}{\sqrt{\partial \mathcal{Y}/\partial x_j \partial \mathcal{Y}/\partial x_j}}, \tag{1.5}$$

$$\kappa = \frac{\partial n_i}{\partial x_i} = -\frac{1}{\sigma}\frac{\partial \sigma}{\partial s}. \tag{1.6}$$

In turbulent premixed combustion the total fuel consumption is a result of the combined effect of flame surface increase and local modulation of the mass burning rate. In the present study the latter will be investigated on the basis of Eq. 1.3 and possible parameterizations thereof, i.e. models for the Karlovitz integral, Eq. 1.4.

2. Methodology

In this section the governing equations and the numerical treatment are presented. Followed by the construction of the initial fields.

2.1. *Numerical method*

Freely expanding flames are modelled in a turbulent flow field using DNS. More detailed information about the DNS program can be found in Bastiaans *et al.* (2001) and Groot (2003). The governing equations are,

$$\frac{\partial \rho}{\partial t} + \frac{\partial}{\partial x_i}(\rho u_i) = 0$$

$$\rho \frac{\partial u_j}{\partial t} + \rho u_i \frac{\partial u_j}{\partial x_i} = -\frac{\partial p}{\partial x_j} + \frac{\partial \sigma_{ij}}{\partial x_i}$$

$$\rho \bar{c}_v \frac{\partial T}{\partial t} + \rho u_i \bar{c}_v \frac{\partial T}{\partial x_i} = \frac{\partial}{\partial x_i}\left(\lambda \frac{\partial T}{\partial x_i}\right) - p\frac{\partial u_i}{\partial x_i} + \sigma_{ij}\frac{\partial u_i}{\partial x_j} +$$
$$\Sigma_\alpha \left[[R_\alpha T - h_\alpha]\dot{\rho}_\alpha + \rho R_\alpha T D_{\alpha m} \frac{\partial^2 Y_\alpha}{\partial x_i^2} + \frac{\partial Y_\alpha}{\partial x_i}\frac{\partial \rho R_\alpha T D_{\alpha m}}{\partial x_i} - \rho D_{\alpha m}\frac{\partial Y_\alpha}{\partial x_i}\frac{\partial [R_\alpha T - h_\alpha]}{\partial x_i} \right]$$

$$\rho \frac{\partial Y_\alpha}{\partial t} + \rho u_i \frac{\partial Y_\alpha}{\partial x_i} = \frac{\partial}{\partial x_i}\left(\frac{\lambda}{Le_\alpha \bar{c}_p}\frac{\partial Y_\alpha}{\partial x_i}\right) + \dot{\rho}_\alpha \tag{2.1}$$

with

$$\sigma_{ij} = \mu\left(\frac{\partial u_i}{\partial x_j} + \frac{\partial u_j}{\partial x_i} - \frac{2}{3}\delta_{ij}\frac{\partial u_k}{\partial x_k}\right); \qquad p = \rho R T. \tag{2.2}$$

The viscosity of the mixture is computed with Sutherland's law and the ratio of the thermal conductivity and the heat capacity at constant pressure (λ/c_p) is assumed to be a function of temperature only (Smooke & Giovangigli 1991). The species heat capacities are tabulated in polynomial form. Unity Lewis numbers are assumed for all species in order to prevent differential diffusion effects from obscuring the direct effects of stretch and curvature on the mass burning rate.

The equations are in fully compressible form and are solved in a three-dimensional cubic computational domain with a length of 12 mm and 254 grid points uniformly distributed in each direction. This gives a mesh size of approximately 0.0472 mm in each direction. For the spatial discretization of second derivatives, the sixth order accurate compact finite difference method of Lele (1992) is used. First order derivatives connected to advection are treated by a compact fifth order finite difference method, developed by De Lange (2004). The time integration is performed explicitly with a compact storage third-order Runge-Kutta method. A time step of order 10^{-8} is used to satisfy the stability criteria.

The boundary conditions are modelled with the Navier-Stokes Characteristic Boundary Conditions (NSCBC) of Poinsot & Lele (1992). The initial flame kernels are expanding at atmospheric conditions, which means that all boundaries of the cubic computational domain are modelled as outlet boundaries to prevent pressure build-up in the domain. Therefore, partially-reflecting outlet boundaries are required, imposing a fixed pressure far away.

To make the DNS computations affordable, the FGM method of Van Oijen (2002) is used to describe the reaction kinetics. FGM can be considered a combination of the flamelet approach and the intrinsic low-dimensional manifold (ILDM) method of Maas & Pope (1992) and is similar to the Flame Prolongation of ILDM (FPI) introduced by Gicquel *et al.* (2000). FGM is applied similarly to ILDM. However, the thermo-chemical data-base is not generated by applying the usual steady-state relations, but by solving a set of 1D convection-diffusion-reaction equations describing the internal flamelet structure. The main advantage of FGM is that diffusion processes, which are important near the interface between the preheat zone and the reaction layer, are taken into account. This leads to a very accurate method for (partially) premixed flames that uses fewer controlling variables than ILDM. The manifold used in this paper is based on the GRI3.0 kinetic mechanism with 53 species and 325 reversible reactions (Smith *et al.* 1999).

The mass fraction of carbon dioxide, which is monotonically increasing, is used as the single controlling variable (progress variable). Since pressure, enthalpy and element mass fractions are constant in these flames, they are not needed as additional controlling variables. A large portion of the terms and parameters in the governing equations, Eq. 2.1, are given by the manifold. These items include the source term for the progress variable, the source term for the temperature equation, which is given by all the terms in the summation over species (the large term in square brackets), the viscosity, conductivity, specific gas constant, the heat capacity at constant volume and the ratio of heat capacities.

2.2. *Initial conditions*

The initial conditions are a laminar spherical flame superimposed on a turbulent field. There is no forcing in the simulation, so the turbulence will decay in time. In order to select a physical condition to be considered one normally refers to a certain region of the premixed combustion regime diagram given by (Peters 2000) among others. Given a certain chemistry, the regime is given by the applied turbulence in terms of the amplitude

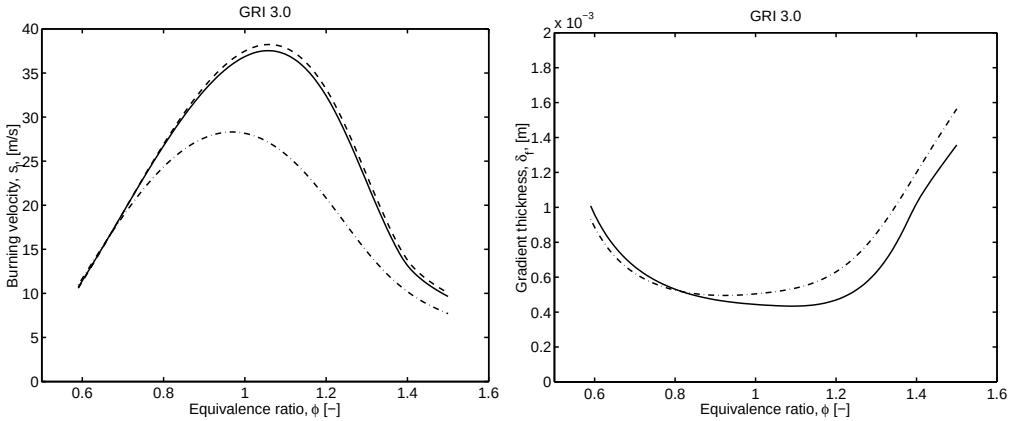

FIGURE 1. Burning velocity and flame gradient thickness from simulation of laminar methane air combustion as function of equivalence ratio based on GRI3.0 at 300 K and $1.013250{\cdot}10^5$ Pa. Left: Burning velocity using full GRI3.0 kinetics (drawn line), mixture average Lewis numbers approximation (dashed) and $Le_i = 1$ approximation (dash-dotted). Right: Flame gradient thickness, full GRI3.0 (drawn) and $Le_i = 1$ approximation (dash-dotted).

of the velocity fluctuations and the mean turbulent coherence length given by the Taylor integral scale. The procedure to initialize the turbulence starts with drawing random numbers for a stream function. This field is subsequently filtered multiple times by means of a top-hat filter. This results in a smooth field in which derivatives can be approximated with sufficient accuracy and a certain Taylor scale depending on the number of filter operations. It must be remarked that the number of filter operations generally is of the order of 100, so that the effective filter is an accurate approximation of a Gaussian. In order to keep disturbances away from the domain boundaries, the resulting field is windowed with a tanh function, decreasing from 1 to 0 at a diameter of 0.8 times the domain size and with a width of 0.05 times the domain size. Subsequently, derivatives are taken from the stream function to obtain the velocity components of a solenoidal field.

The chemistry is chosen due to the large interest in the power industry in lean premixed combustion engines and there is detailed knowledge of its chemical kinetics. Therefore premixed combustion of a methane/air mixture is used, with an equivalence ratio of $\phi = 0.7$. An additional advantage for lean methane chemistry is that the flame speed and the flame thickness are equal for the full GRI3.0 kinetics, and for the case in which these kinetics are used with a $Le_i = 1$ approximation (as can be observed from simulations using CHEM1D (2002), displayed in figure 1). We will use the $Le_i = 1$ approximation in the present study. The advantage is that the results will not be obscured by differential diffusion effects.

Our objective is to analyse the flame dynamics in a well defined and sufficiently resolved case. The most interesting region in the regime diagram with respect to the objective of the present study is the transition from the thin reaction zones regime towards the distributed reactions zone regime. It is expected that somewhere in this region the FGM method (as used in the present mode with only one progress variable, based on the ratio of the CO_2 mass fraction and its equilibrium value) loses its validity. In this study we will restrict ourselves to conditions where the use of just one progress variable is still a good assumption. Additionally, the simulations are constrained by geometrical and numerical conditions.

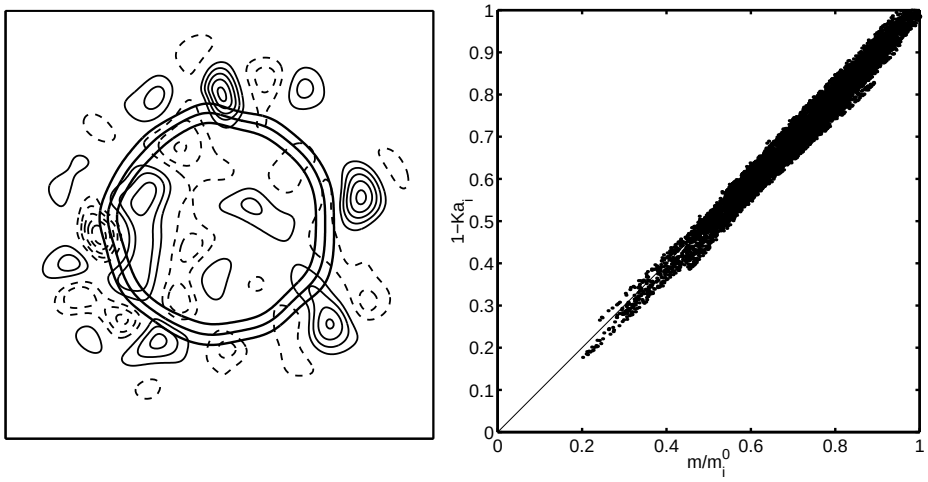

FIGURE 2. Case C1, left: Vorticity contours (positive and negative values indicated by solid and dashed lines, respectively) and progress variable (thick lines, values 0.2, 0.5, 0.8), right: Correlation of the actual mass burning rate with the basic model (result of 52000 flamelets found in the domain).

Since the domain size depends on the starting field of the controlling variable (progress variable), a relevant initial flame kernel must be chosen. For this reason and for comparison of turbulent results with a laminar undisturbed flame development, the evolution of the initial laminar spherical flame kernel is calculated with detailed chemistry as well. Again, the CHEM1D (2002) code was used, but now using spherical coordinates. The starting condition is a flat adiabatic flame at the same conditions, which is converted geometrically to a spherical flame with a very small radius. It is assumed that this kernel adjusts itself in time to a sort of self-similar laminar flame kernel.

3. Results

In this section the test cases are presented, followed by the flamelet analysis. The section closes with the presentation of results.

The first simulation, denoted C1, is a lean case with an equivalence ratio of $\phi = 0.7$, domain size of 12 mm, an initial flame kernel radius of approximately 2.9 mm, turbulent fluctuations of $u' = 0.4$ m/s and a turbulence length scale of ℓ_t=1.15 mm. In order to allow for very mild perturbations, initially we study the results at a time equal to 0.026τ, with $\tau = \ell_t/u' = 2.9ms$, taken from the start of the simulation. The time of growth of the laminar flame kernel to the initial DNS size was about 5 ms. The burning velocity of a flat unstretched flame with respect to the unburnt mixture is equal to $s_L^0 = 18.75$ cm/s and the corresponding mass burning rate is $m^0 = 0.213$ kg/m^{2}s. The progress variable is taken to be the carbon dioxide mass fraction, normalized with the maximum adiabatic value. At the left side of figure 2 is a cross section of the field. The contours of the progress variable are deformed only very mildly. It is observed that the scale of the vorticity patches are larger then the integral flame thickness. For this field the mass burning rate is analyzed as a reference case.

Additional analyses are performed in order to assess the basic model (Eq. 1.4) under varying physical conditions. The test cases are listed in table 1. In case C2, the effect of

Case	ϕ	u' $[m/s]$	ℓ_t $[mm]$	δ_f $[mm]$	L $[mm]$	r_{ini} $[mm]$	grid	$Re_t = u'\ell_t/s_L^0\delta_f$	tu'/ℓ_t
C1	0.7	0.40	1.15	0.614	12	2.9	254^3	4.0	0.026
C2	0.7	0.40	1.15	0.614	12	2.9	125^3	4.0	0.026
C3	1.0	0.60	0.89	0.475	12	2.9	254^3	4.0	0.026
C4	0.7	0.70	0.77	0.614	20	3.9	254^3	4.7	0.026
C5	0.7	1.31	0.94	0.614	12	2.9	254^3	10.7	0.026
C6	0.7	1.30	0.66	0.614	12	2.9	254^3	7.5	0.026

TABLE 1. Physical properties correspondig to the different simulations

grid resolution is investigated. It is assumed that the FGM method is valid in the flamelet regime if the progress variable is approximated with enough accuracy. Since all lengths scales of the gradients of primary variables (i.e. the variables that are solved in the present DNS calcualations) are of the same order, this will yield satisfactory solutions. In order to assess the influence of the chemistry a stoichiometric case, C3, is selected, in which the same ratio of the turbulent velocity fluctuations compared to the laminar flame speed, and the turbulent integral length scale compared to the initial flame thickness as used for cases C1 and C2. For the stoichiometric case at unity Lewis numbers the burning velocity is $s_L^0 = 28.17$ cm/s and the corresponding mass burning rate is $m^0 = 0.316$ kg/m^{2}s. An additional case is given by the simulation of an increased initial flame kernel in a larger domain, C4. Here also the effective resolution is decreased. In addition, cases are chosen with increased velocity fluctuations and decreased length scales, cases C5 and C6, respectively.

In the analysis, the stretch rate defined by,

$$\rho K = \frac{\partial}{\partial x_i}(\rho s_L n_i), \tag{3.1}$$

is evaluated by using the relation for the local burning velocity s_L,

$$s_L = \frac{\left(\frac{\partial}{\partial x_i}\left(\frac{\lambda}{Le\bar{c}_p}\frac{\partial \mathcal{Y}}{\partial x_i}\right) + \dot{\rho}\right)}{\left|\frac{\partial \mathcal{Y}}{\partial x_i}\right|}, \tag{3.2}$$

which is a consequence of the combination of the conservation equation for $\mathcal{Y}$ with the kinematic equation for $\mathcal{Y}$. The latter defines the flame speed u_{if} and then the relation for the flame velocity, $u_{if} = u_i + s_L n_i$, can be used to arrive at Eq. 3.2.

Now the actual mass burning rate can be compared to model-values. This is performed by looking for points in the domain that are close to the inner layer and interpolate from there in the direction of positive and negative gradient of the progress variable, with steps of 1/20 times the gridsize. All relevant variables are interpolated over these flamelets and these flamelets are analysed to determine the burning velocity of Eq. 3.2 and the model of the mass burning rate given by Eq. 1.4. For the present simulations these analyses lead to lots of starting points (e.g. for case C1: 52000) and thus resulting flamelets. For case C1 the correlation is depicted on the right side of figure 2. This shows that the model is a relatively accurate description of the actual mass burning rate. Deviations of the actual

Case	C1	C2	C3	C4	C5	C6
Mean	0.0072	0.0081	0.0075	0.0091	0.0107	0.0094
RMS	0.0215	0.0202	0.0216	0.0236	0.0336	0.0280

TABLE 2. Differences of the mass burning rate with the basic model.

mass burning rate compared to the model (Eq. 1.4) are given in table 2 for all six cases. It is seen that the mean error for all cases is about 0.01 or less, with a root mean square value of 0.02 to 0.03 (without normalization). It can be concluded that the model is a good description for all the present cases. Moreover, the grid coarsening shows no real deterioration, indicating that all cases are sufficiently resolved.

Starting from this point approximations to Eq. 1.4 can be considered. First, one can consider the case in which the surface area is taken to be constant, $\sigma = \sigma_{\rm in}$ as used frequently in the literature,

$$\mathcal{K}a'_{\rm in} := \frac{1}{m^0_{\rm in}} \left(\int_{s_u}^{s_b} \rho K \mathcal{Y} ds - \int_{s_{\rm in}}^{s_b} \rho K ds \right). \tag{3.3}$$

An improved model can be constructed by assuming that the curvature is not a function of the distance s, but that it remains constant equal to the inner layer value $\kappa = \kappa_{\rm in}$. By integrating Eq. 1.6 this yields for the surface

$$\sigma = \exp\left(-\kappa_{\rm in}(s - s_{\rm in})\right). \tag{3.4}$$

A third approximation is that the iso-planes of the progress variable are concentric, either cylindrical or spherical yielding

$$\sigma = \left(\frac{\xi/\kappa_{\rm in} - s}{\xi/\kappa_{\rm in}} \right)^{\xi}, \tag{3.5}$$

in which ξ takes the value 2 for spherical curvature and 1 for cylindrical curvature. This has to be limited for distances s beyond the concentric origin, $s > \xi/\kappa_{\rm in}$, at which $\sigma = 0$.

The result of the approximations are given in table 3 for all cases. It is observed that the constant flame surface conjecture gives rise to relatively large error. There is a systematic over-prediction of about 0.05 (without normalization) of the mass burning rate with this model and the fluctuations are of the same order of magnitude. The other approximations give much better results. For the mean differences the spherical approximation, $\xi = 2$, is superior compared to the cylindrical model, $\xi = 1$, and for most cases also compared to the constant curvature model. However, this is not really substantiated when looking at the accompanying fluctuations. For the better resolved cases, C1 and C3, the mean difference is best predicted by the $\xi = 2$ model, but again the accompanying fluctuations are much larger than the model deviation. This suggests that it is not a real improvement. With respect to the fluctuations it seems that constant curvature gives the smallest deviations. Additionally, it can be observed that the constant curvature estimation gives slight under-predictions, whereas the concentric cases give systematic increased values of the mass burning rate. Moreover it can be seen that the stoichiometric case (C3) gives

Case	C1	C2	C3	C4	C5	C6
$\sigma = \sigma_{\text{in}}$						
Mean	-0.0537	-0.0519	-0.0340	-0.0496	-0.0653	-0.0810
RMS	0.0552	0.0473	0.0373	0.0641	0.0772	0.1004
$\kappa = \kappa_{\text{in}}$						
Mean	0.0062	0.0055	0.0029	0.0026	0.0082	0.0079
RMS	0.0103	0.0085	0.0055	0.0173	0.0186	0.0338
$\xi = 2$						
Mean	-0.0011	-0.0006	-0.0007	-0.0075	-0.0037	-0.0141
RMS	0.0114	0.0101	0.0074	0.0313	0.0224	0.0540
$\xi = 1$						
Mean	-0.0059	-0.0050	-0.0032	-0.0115	-0.0101	-0.0219
RMS	0.0169	0.0142	0.0098	0.0333	0.0281	0.0556

TABLE 3. Differences of the mass burning rate determined by the basic model compared to the approximations.

the smallest deviations for any of the present approximations. This indicates that the choice of progress variable for the lean case might not be the best choice.

For closer inspection of all realizations in the field, case C6 is chosen in which the deviations are largest. Correlation plots are shown in figure 3. For this case the basic model does not deviate significantly from the results in figure 2, the only difference being that the range of values is extended more to the origin of the plot. Moreover some features, as indicated above, are clearly reflected like the under-prediction of the constant surface case. Furthermore the predictions of the concentric cases are less robust compared to the constant curvature model. The latter however gives deviations at small mass burning rates. This is also observed, to a lesser degree, in the concentric spherical approximation. Near the origin the cylindrical model seems to perform better. This is in agreement with observations of Jenkins & Cant (2002), who found that at higher turbulence levels, curvature in premixed turbulent combustion of flame kernels tends to cylindrical modes of deformation of the flame front.

It is obvious that all models do not fit to the true values because no local information on the flame geometry is taken into account in the approximations. If local geometric information is taken into account a much better agreement would be possible and will be a topic of further research. At larger times in the evolution, e.g. case C6, it was found that the basic model Eq. 1.4, gives good correlations (at $t = 0.087\tau$ mean deviation 0.08, rms values of 0.24), see figure 4, whereas all approximations are starting to deteriorate

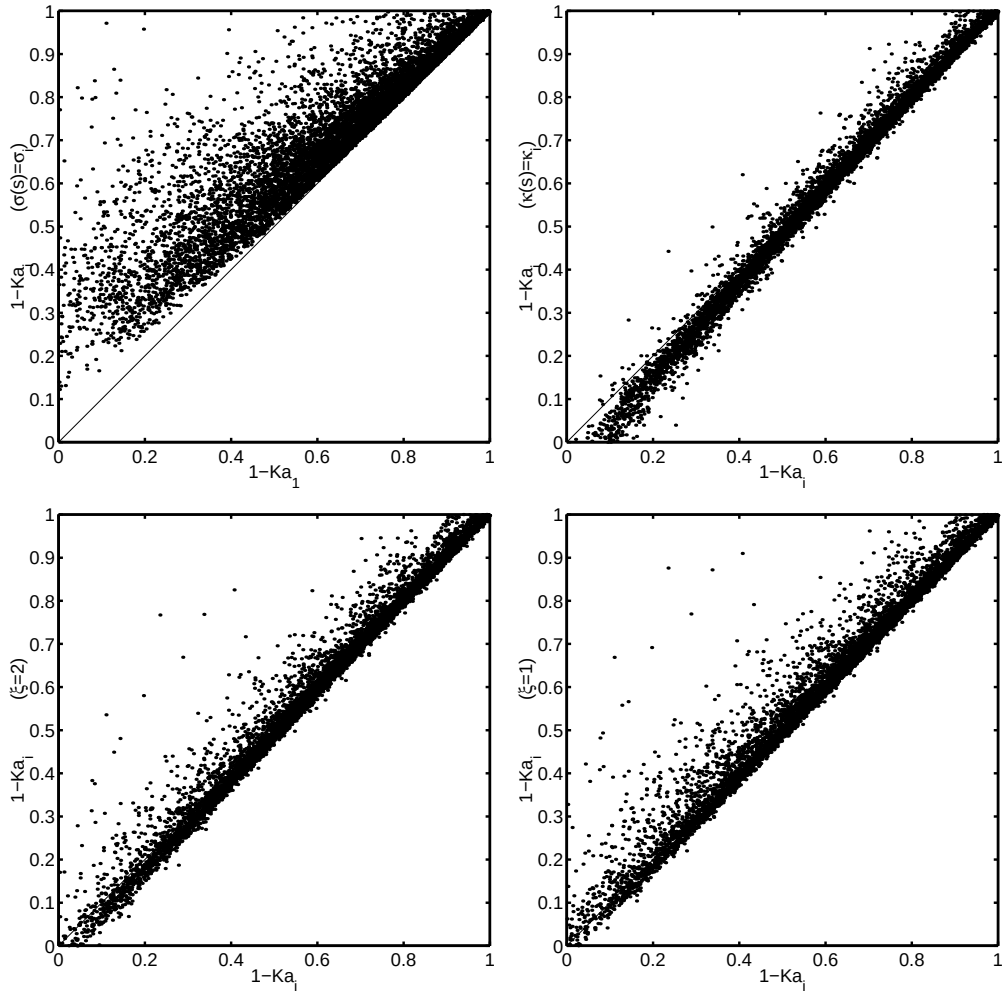

FIGURE 3. Case C6, Correlation of the actual mass burning rate with the approximations, top left: $\sigma = \sigma_{\rm in}$, top right: $\kappa = \kappa_{\rm in}$, bottom left: $\xi = 2$, bottom right: $\xi = 1$ (result of 60000 flamelets found in the domain).

severely. In this case the curvatures have large values, the associated values of radii are within the flame thickness, $\delta_{\rm f}$, as shown in the figure (at the right).

4. Future plans

From the previous results it can be concluded that the method of FGM in combination with DNS calculations looks very encouraging. It appears that the FGM is a promising technique to reduce the chemistry and obtain accurate results for the flow, thermodynamics and species. However, apart from a validation in terms of laminar burning velocity, a direct validation is not present for turbulent cases. With respect to this, more validation is needed and the strategy for this will be twofold. By applying a suitable kinetics model with a limited number of species, a DNS can be conducted. This system can be reduced and validated directly against the results of the detailed chemistry calculations. A sec-

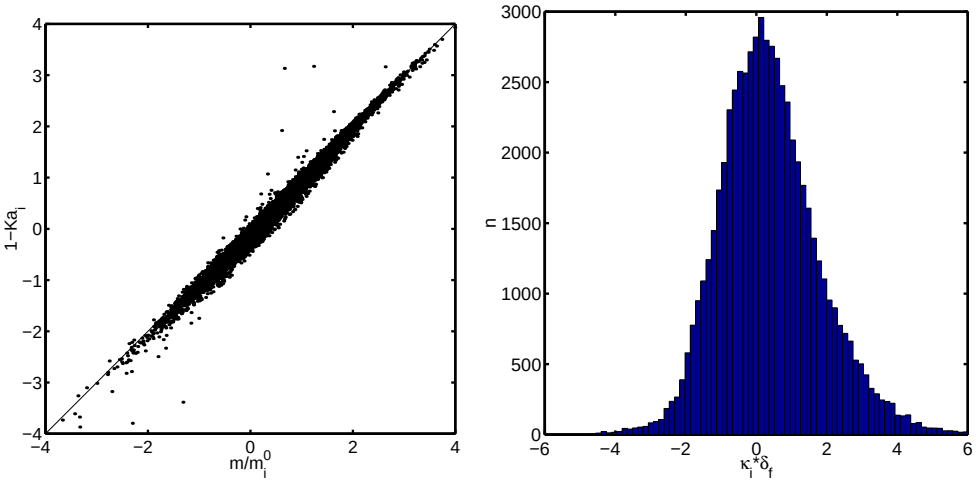

FIGURE 4. Results of case C6 at time $t = 0.087\tau$, left: correlation of the actual mass burning rate with the basic model, right: PDF of inner layer curvatures.

ond method is to increase the dimension of the manifold. It must be studied how many controlling variables are required for a certain accuracy of the predictions. This again can be performed in the framework of the previously mentioned full chemistry DNS.

REFERENCES

BASTIAANS, R. J. M., SOMERS, L. M. T. & DE LANGE, H. C. 2001 DNS of non-premixed combustion in a compressible mixing layer. In B.J. Geurts, editor, *Modern Simulation Strategies for Turbulent Flow*, R.T. Edwards Publishers, Philadelphia, 247-261.

BELL, J. B., DAY, M. S. & GRCAR, J. F. 2002 Numerical simulation of premixed turbulent methane combustion. *Proc. Comb. Inst.*, **29**, 1987-1993.

BRAY, K. N. C. & MOSS, J. B. 1977 A unified statistical model of the premixed turbulent flame. *Acta Astronautica*, **4**, 291-319.

CHEM1D 2002 A one dimensional flame code. Eindhoven University of Technology, http://www.combustion.tue.nl/chem1d.

DRISCOLL, J.F. 2003 Premixed Turbulent Combustion - Current Knowledge and New Challenges. *Invited Presentation at the 3rd Joint Meeting of the U.S. Sections of the Combustion Institute*, Chicago (IL), March 16, 2003.

GASHI, S., HULT, J., JENKINS, K.W., CHAKRABORTY, N., CANT, R.S. & KAMINSKI, C.F. 2004 Curvature and wrinkling of premixed flame kernels - comparisons of OH PLIF and DNS data. *Proc. Comb. Inst.*, **30**, In press.

GICQUEL, O., DARABIHA, N. & THEVENIN, D. 2000 Laminar premixed hydrogen/air counter flow flame simulations using flame propagation of ILDM with preferential diffusion. *Proc. Combust. Inst.* **28**, 1901-1908.

DE GOEY, L. P. H. 2000 Premixed turbulent combustion theory. Technical report, TUE-W, sabbatical visit at the RWTH-Aachen

DE GOEY, L. P. H. & TEN THIJE BOONKKAMP, J. H. M. 1997 A mass-based definition of flame stretch for flames with finite thickness. *Comb. Sci. Tech.*, **122**, 399-405.

DE GOEY, L. P. H. & TEN THIJE BOONKKAMP, J. H. M. 1999 A flamelet description of premixed laminar flames and the relation with flame stretch. *Comb. Flame*, **119**, 253-271.

DE GOEY, L. P. H., PLESSING, T., HERMANNS, R. T. E. & PETERS, N. 2004 Analysis of the flame thickness of turbulent flamelets in the thin reaction zones regime. In *Proc. Combust. Inst.*, **30** In press.

GROOT, G. R. A. 2003 Modelling of propagating spherical and cylindrical premixed flames. Ph.D. thesis, Eindhoven University of Technology.

GROOT, G. R. A. & DE GOEY, L.P.H. 2002 A computational study of propagating spherical and cylindrical premixed flames. *Proc. Combust. Institute*, **29**, 1445-1451.

JENKINS, K.W. & CANT, R.S. 2002 Curvature effects on flame kernels in a turbulent environment. *Proc. Comb. Inst.*, **29**, 2023-2029.

DE LANGE, H. C. 2004 Personal communication Eindhoven University of Technology.

LELE, S. K. 1992 Compact Finite Difference Schemes with Spectral-like Resolution. *J. Comput. Phys.* **103**, 16-42.

MAAS, U. & POPE, S. B. 1992 Simplifying Chemical Kinetics: Intrinsic Low-Dimensional Manifolds in Composition Space. *Combust. Flame* **88**, 239-264.

MARBLE, F. & BROADWELL, J. 1977 The coherent flame model for trubulent chemical reactions. TRW-9-PU Project Squid, Purdue University West Lafayette.

VAN OIJEN, J.A. 2002 Flamelet-Generated Manifolds: Development and Application to Premixed Laminar Flames. Ph.D. thesis, Eindhoven University of Technology, The Netherlands.

VAN OIJEN, J. A. & DE GOEY, L. P. H. 2002 Modelling of premixed counterflow flames using the flamelet-generated manifold method. *Combust. Theory Modelling*, **6**, 463-478.

VAN OIJEN, J. A., GROOT, G. R. A., BASTIAANS, R. J. M. & DE GOEY, L. P. H. 2004 A flamelet analysis of the burning velocity of premixed turbulent expanding flames. *Proc. Comb. Inst.*, **30**, In press.

POINSOT, T. J. & S. K. LELE 1992 Boundary Conditions for Direct Simulations of Compressible Viscous Flows. *J. Comput. Phys.* **101**, 104-129.

PETERS, N. 2000 *Turbulent combustion.* Cambridge University Press.

SHEPHERD, I. G., CHENG, R. K., PLESSING, T., KORTSCHIK, C. & PETERS, N. 2002 Premixed flame front structure in intense turbulence. *Proc. Comb. Inst.*, **29**, 1833-1840.

SMITH, G. P., GOLDEN, D. M., FRENKLACH, M., MORIARTY, N. W., EITENEER, B., GOLDENBERG, M., BOWMAN, C.T., HANSON, R. K., SONG, S., GARDINER JR., W. C., LISSIANSKI, V.V. & Z. QIN, Z. 1999 http://www.me.berkeley.edu/gri_mech/

SMOOKE, M. D. & GIOVANGIGLI V. 1991 Formulation of the Premixed and Non-premixed Test Problems. In *Lecture Notes in Physics*, **384**, 1-28.

THÉVENIN, D. 2004 Three-dimensional direct numerical simulations and structure of expanding turbulent methane flames. *Proc. Comb. Inst.*, **30**, In press.